# Quasi-Chemical Theory for Anion Hydration and Specific Ion Effects: $Cl^-(aq)$ *vs.* $F^-(aq)$

A. Muralidharan[a], L. R. Pratt[a], M. I. Chaudhari[b], S. B. Rempe[b] †

*amuralid@tulane.edu, lpratt@tulane.edu, michaud@sandia.gov, slrempe@sandia.gov*

[a] *Department of Chemical and Biomolecular Engineering, Tulane University, New Orleans, LA 70118, U.S.A.*
[b] *Department of Nanobiology, Sandia National Laboratories, Albuquerque, NM 87185, U.S.A.*
† *Corresponding author: 505-845-0253*

arXiv:1907.07644v1 [physics.chem-ph] 17 Jul 2019

**Abstract**

Anion hydration is complicated by H-bond donation between neighboring water molecules in addition to H-bond donation to the anion. This situation can lead to competing structures for chemically simple clusters like $(H_2O)_nCl^-$ and to anharmonic vibrational motions. Quasi-chemical theory builds from electronic structure treatment of isolated ion-water clusters, partitions the hydration free energy into inner-shell and outer-shell contributions, and provides a general statistical mechanical framework to study complications of anion hydration. The present study exploits dynamics calculations on isolated $(H_2O)_nCl^-$ clusters to account for anharmonicity, utilizing ADMP (atom-centered basis sets and density-matrix propagation) tools. Comparing singly hydrated $F^-$ and $Cl^-$ clusters, classic OH-bond donation to the anion occurs for $F^-$, while $Cl^-$ clusters exhibit more flexible but dipole-dominated interactions between ligand and ion. The predicted $Cl^-$ – $F^-$ hydration free energy difference agrees well with experiment, a significant theoretical step for addressing issues like Hofmeister ranking and selectivity in ion channels.

*Keywords:* QCT, hydration, clusters, anions, chloride, fluoride, ADMP

## 1. Introduction

Here, we build a fundamental molecular statistical mechanical theory for hydration of chloride ion ($Cl^-$). Theory of the type targeted here, specifically quasi-chemical theory (QCT), permits transparent comparison of $Cl^-$ to analogous cases such as fluoride hydration ($F^-$). Comparisons of that sort underpin specific ion effects in areas of broad current interest, including the Hofmeister ranking [1–6] of ions and the mechanism of specific ion permeation in membrane ion channels. An example of membrane ion channels is the CLC family, which regulate membrane transport of $Cl^-$.[7] Though we comment further below on such long-term goals, we focus primarily on extending QCT to hydrated anions. One motivation for comparisons such as $Cl^-$ with $F^-$ is that they permit rigorous experimental thermodynamic testing of single-ion free energies without discussion of potentials of the phase,[8,9] or surface potentials.[10–12]

Adequate molecular simulation is necessary for compelling molecular statistical thermodynamic theory of liquid solutions, and extensive simulation studies have been carried out.[13–22] Available computational work has nicely delineated distinctions in hydration structure of anions compared to simple metal ions, and distinctions between different halide ions.[23–26] In this crowded landscape of computational work, molecular-scale statistical mechanical theory for these systems has been meager, with striking exceptions.[27]

Quasi-chemical theory (QCT), in the present incarnation based on clusters,[28,29] provides a natural starting point for the theory sought.[6,30] QCT[28,29,31–35] naturally divides the free energy determination into inner-shell and outer-shell considerations, as is apparent from Eq. (1) below. In this approach, the necessary contributions are physically meaningful,[36] and can then be evaluated to the desired accuracy — even judiciously using experimental results for natural intermediate results.[37] QCT, considered broadly over nearly two decades, has been applied successfully to a wide range of systems, including the hard sphere fluid,[38] liquid water,[35,36,39], small molecule solvation[40–45] also involving ion channels[46–49] and other macromolecules,[50–52] cations in water and non-aqueous solvents,[32,53–62] and biomolecule hydration.[63,64]

The QCT approach provides a complete statistical mechanical framework for evaluating solvation free energies of ions by building up from carefully defined isolated ion-solvent clusters.[28] Experimental measurements addressing the energetics of such clusters, based on mass spectroscopy,[65–67] have existed for some decades. For hydrous clusters, a compilation of those experimental values are available from Tissandier, *et al.*[68]

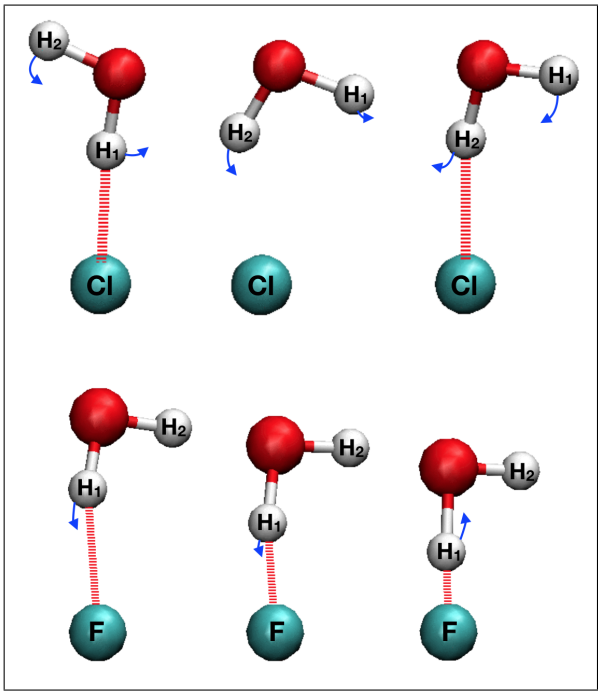



Figure 1: Sequence of structures over about 0.1 ps of the ADMP classical dynamics calculations. An animated display is available at (`https://doi.org/10.6084/m9.figshare.8066270`) and discussed in Section 3.3. The qualitative impression is of $(H_2O)\,Cl^-$ (upper) rocking through a dipole-dominated configuration, in contrast to (lower) OHF stretching vibration for the $(H_2O)\,F^-$ cluster.

QCT has been applied less to the challenging cases of anion hydration than to metal cations, comparatively. A primary difficulty is hydrogen bonding between water molecules of clusters such as $(H_2O)_nCl^-$, leading to structures that are less susceptible to simple approximation in the implementation of QCT. Recent efforts have been directed toward addressing those initial approximations in the application of QCT. Some of the refinements include quantification of anharmonic effects[37,41,44,48] on free energies of solute-water clusters and the sufficiency of the polarizable continuum model[41,60,69] (PCM) for the hydration free energy of those clusters.

Anticipating results below (Section 3.2), a harmonic approximation to the potential energy surface of $(H_2O)_nCl^-$ clusters is satisfactory for cluster formation enthalpies, but not for free energies. To investigate such issues, we use a molecular dy-

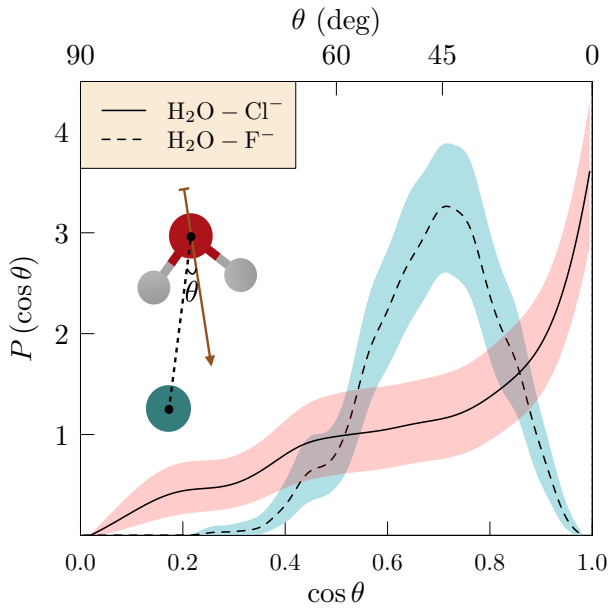



Figure 2: Distribution of $\cos\theta$, with $\theta$ the angle between water dipole moment and the $OX^-$ vector, observed over the last 5 ps of a 10 ps ADMP trajectory at $T$=300 K. For $H_2O-F^-$, the distribution peaks at 45° with an OH bond oriented toward the $F^-$, as shown in Figure 1. In contrast, the $\theta$ distribution spans from 0° to 90°, with maximum near 0°, for $H_2O-Cl^-$. Rocking through dipole-dominated configurations allows the water molecule to offer alternate H atoms for coordination with the ion. The filled bands indicate approximate 99% confidence intervals, estimated on the basis of a resampling (bootstrap) procedure.

namics approach that explicitly includes electron coordinates, as we now discuss.

Classical trajectory calculations that include electron coordinates fall into two major categories: Born-Oppenheimer (BO) molecular dynamics (MD) and extended Lagrangian (EL) dynamics. In the BO approach, the atomic dynamics develop on a potential energy surface obtained from an optimized-in-detail electronic structure calculation. In EL approaches such as Car-Parrinello molecular dynamics (CPMD),[70] electron coordinates are introduced as fictitious dynamic variables that couple electronic and atomic motion. The dynamics should keep the fictitious electronic degrees of freedom near the ground state BO potential energy surface, yielding sufficiently accurate forces for the atomic trajectory.

The *atom-centered basis sets and density matrix propagation* (ADMP)[71] tool is an extended Lagrangian approach for molecular dynamics. In contrast with CPMD, ADMP emphasizes finite non-periodic systems, and thus is convenient for the isolated clusters of interest here (Figure 1). ADMP has been shown to provide similar functionality to BO molecular dynamics.[71]

### *1.1. Perspective from interest in $Cl^-$ and $F^-$ ion channels*

The regulation of ion concentration is essential for several physiological functions in cells.[72] For anions such as $Cl^-$, this control is achieved through membrane channels and transport proteins from the CLC family, which facilitate the passage of $Cl^-$ through electro-chemical potential gradients.[7] Numerous efforts[73–76] have been directed toward deciphering the structures of those proteins and understanding their functional characteristics, such as conductance, gating, and ion selectivity.

While CLC proteins select for $Cl^-$, other channel proteins discriminate against $Cl^-$. An interesting example is FLUC, a family of fluoride-specific ion channels with dual-topology architecture.[77] These channels display an astonishingly high selectivity of $10^4$ for $F^-$ over $Cl^-$ despite close similarity in size and identical charge of the ions. FLUC channels provide a ladder of hydrogen-bond donating residues that apparently create a polar track for $F^-$. How that polar track leads to the unusually high level of discrimination between $F^-$ and $Cl^-$ remains an open question. Understanding such mechanisms for selectivity in ion transport has been a primary target for many recent modeling and simulation studies, emphasizing $K^+/Na^+$ selectivity of potassium ion channels.[46,47,50,78–92] But computational studies of anion transport mechanisms demonstrated by CLC channels[93–99] that address comparison to alternatives such as FLUC are less mature.

To address ion selectivity between different media, a rigorous treatment would require comparison of the total free energy of ion solvation between those environments. However, ion channels are thought to function primarily by manipulation of the local environment of the ion. That manipulation may arise from constraints on local structure imposed by the structural and chemical properties of the surrounding environment or the binding sites on the channel itself.[29,46–50,52,57,79,80,82,100] Furthermore, contributions to solvation free energy from long-ranged electrostatic interactions between an ion and the distant environment might cancel between ions of the same charge. Therefore, analysis of selectivity might not require a detailed description of the long-ranged interactions in the molecular theory. Instead, rigorous treatment of local interactions are likely important for accurate treatment of ion selectivity.

Here, we compare the hydration of $Cl^-$ with $F^-$, focusing on rigorous evaluation of local interactions. Broader issues such as the Hofmeister ranking of ions and selectivity in membrane channels are reserved for the future. In the next two sections we lay out the theory and results, followed by a concluding discussion. The details of the numerical implementation are specified in Section 5.

## 2. Theory: Step-wise evaluation of the isolated cluster free energy

QCT formulates the net hydration free energy as

$$\mu_{X^-}^{(ex)} = -RT \ln K_n^{(0)} {\rho_{H_2O}}^n + RT \ln p_{X^-}(n) + \left( \mu_{(H_2O)_n X^-}^{(ex)} - n\mu_{H_2O}^{(ex)} \right) , \quad (1)$$

collecting the individual quasi-chemical contributions.[28,29] The first and last term represent the inner-shell and outer-shell contributions defined based on assignment of a clustering radius ($\lambda$). $p_{X^-}(n)$ then identifies the thermal probability of observing $n$ waters within that prescribed $\lambda$. The several features of this expression will be identified in the following discussion.

To that end, consider the chemical process

$$n H_2O + X^- \overset{K_n^{(0)}}{\rightleftharpoons} (H_2O)_n X^- \quad (2)$$

for formation of the isolated cluster, as in an ideal gas phase (X = Cl here). We seek the free energy (inner-shell) contribution $-RT \ln K_n^{(0)} {\rho_{H_2O}}^n$, with

$$K_n^{(0)} = \frac{\mathcal{Q}(\gamma_n \sigma)/n!}{\mathcal{Q}(\sigma)\left[\mathcal{Q}(\gamma)/V\right]^n} , \quad (3)$$

a classic aspect of statistical thermodynamics.[34,37] Here $V$ is the system volume, $\sigma$ and $\gamma$ represent the solute ($Cl^-$) and solvent ($H_2O$) molecules, respectively, and the $\mathcal{Q}(\gamma_n \sigma)$ are configurational integrals associated with single molecule/cluster canonical partition functions.[37]

Our scheme for evaluating ${K_n}^{(0)}$ proceeds stepwise in $n$ according to

$$\frac{{K_n}^{(0)}}{{K_{n-1}}^{(0)} {K_1}^{(0)}} = \frac{\mathcal{Q}(\gamma_n \sigma)/\mathcal{Q}(\sigma)}{n\left[\mathcal{Q}(\gamma_{n-1}\sigma)/\mathcal{Q}(\sigma)\right]\left[\mathcal{Q}(\gamma\sigma)/\mathcal{Q}(\sigma)\right]} . \quad (4)$$

The numerator on the right of Eq. (4) involves integration carried over canonical distributions of configurations of $n$ solvent molecules, while the denominator treats configurations of $n-1$ and 1, respectively, treated independently. Our scheme is then based on evaluation of

$$\Delta U = E(\gamma_n \sigma) - E(\gamma_{n-1}\sigma) - E(\gamma\sigma) + E(\sigma) , \quad (5)$$

so that

$${K_n}^{(0)} = \frac{{K_1}^{(0)} {K_{n-1}}^{(0)}}{\langle e^{\beta \Delta U} \rangle_n} . \quad (6)$$

The brackets, $\langle \ldots \rangle_n$, indicate the thermal average utilizing configurations from the canonical simulation stream for the $\gamma_n \sigma$ cluster.

For $n = 1$, Eq. (6) reduces to the trivial case of ${K_0}^{(0)} = 1$. In the evaluation of ${K_n}^{(0)}$ for $n \geq 2$, the value of ${K_1}^{(0)}$ can be supplied from experiment[68] or theory. This term describes the interaction between $Cl^-$ and one water molecule. We note that for $(H_2O)Cl^-$, a harmonic approximation gives a sufficiently good estimate for the free energy, but not for bigger cluster sizes (Figure 5). Carrying out subsequent steps in this scheme then addresses the issues that make anion hydration more challenging; that is, the sampling of cluster configurations,[37] including competing H-bonding interactions between neighboring water molecules in those clusters.

Here, we take advantage of the QCT partitioning to evaluate the inner-shell contribution based on accurate quantum mechanical treatment of dynamics (using ADMP) in ion-water clusters. The evaluation of $\left( \mu_{(H_2O)_n Cl^-}^{(ex)} - n\mu_{H_2O}^{(ex)} \right)$ utilizes the same trajectory, but approximates the outer-shell waters using the polarizable continuum model[69] (PCM), as described in section 5. Experimental comparisons (section 7) can then indicate the sufficiency of such an approximation.

## 3. Results

### *3.1. Solution structure*

Neighborship is a fundamental concept in QCT.[28,37,46,59,101] The H-atom of water is the closest neighbor to the anions, $F^-$ and $Cl^-$. Proximity distinctions between those cases are sharper when H atoms are utilized rather than O atoms in the radial distributions. Distributions of water H atoms relative to the ions (Figure 3) then guide the assignment of the clustering radius, $\lambda$. Further, the neighborship-ordered contributions help identify cluster sizes in which waters are always

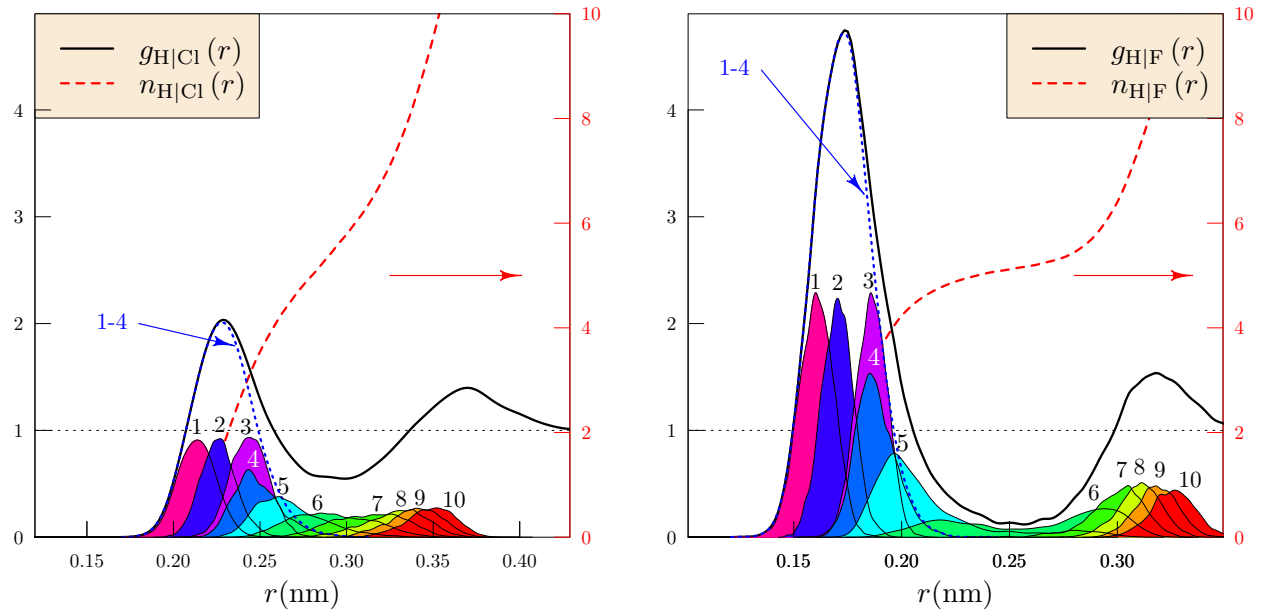



Figure 3: Radial distributions and running coordination number of H atoms relative to $X^-$ from AIMD simulations of $X^-$ in bulk water phase (X = Cl or F). The integer-labeled distributions are the neighborship-ordered contributions of the $n^{\mathrm{th}}$ nearest H atom. A choice $\lambda_{\mathrm{Cl}^-} \leq 0.26$ nm and $\lambda_{\mathrm{F}^-} \leq 0.20$ nm excludes split-shell clusters. Compared to $\mathrm{Cl}^-$(aq), the radial distribution of $\mathrm{F}^-$(aq) displays a larger maximum and a nearly zero first minimum, leading to a distinct plateau of the running coordination number.

in direct contact with the ion. Notice that the distribution of the $6^{\mathrm{th}}$ nearest water around $\mathrm{Cl}^-$ extends beyond the first minimum of $g_{\mathrm{H|Cl}}(r)$. For instance, a choice of $\lambda_{\mathrm{Cl}^-} \leq 0.26$ nm eliminates such split-shell clusters.[46,59,102] The thermal probability ($p_{\mathrm{Cl}^-}(n)$), contributing to the second term of Eq. (1), is then evaluated based on this constraint.

Compared to $\mathrm{Cl}^-$(aq), the radial distribution of $\mathrm{F}^-$(aq) displays a larger maximum and a nearly zero first minimum, leading to a flat behavior of the running coordination number above the minimum (Figure 3). For $\mathrm{F}^-$(aq), this structure suggests tightly bound inner-shell waters, with small deviations from orientations that take the nearest H-atom away from the ion. By comparison, inner-shell waters of $\mathrm{Cl}^-$(aq) are more flexibly structured. The differences highlighted here also feature in the behavior of waters in the gas phase clusters of $(\mathrm{H_2O})_n\,\mathrm{Cl}^-$ and $(\mathrm{H_2O})_n\,\mathrm{F}^-$ (Figures 1 and 2).

### *3.2. Isolated cluster energetics:* $(\mathrm{H_2O})_n\,\mathrm{Cl}^-$

To evaluate cluster energetics, a harmonic approximation was applied initially to the lowest energy geometry-optimized structures (SI, Figure S1). The enthalpies of $(\mathrm{H_2O})_n\,\mathrm{Cl}^-$ cluster calculated this way agree well with experiment (Figure 4). The UPBE1PBE functional with the aug-cc-pvdz basis set showed the best agreement among the two tested functionals. However, the free energy evaluated using the harmonic approximation deviates from experiment, and that deviation increases with $n$ (left panel, Figure 5). We conclude that the entropy of the $(\mathrm{H_2O})_n\,\mathrm{Cl}^-$ cluster is not satisfactorily predicted in our harmonic approximation.

Notice further that the harmonic approximation with the UPBE1PBE functional gives an accurate estimate of free energy for $(\mathrm{H_2O})\,\mathrm{Cl}^-$. Therefore, we expect the discrepancy in the free energy of $(\mathrm{H_2O})_2\,\mathrm{Cl}^-$ to emerge from interactions between water molecules, roughly with an average strength of an H-bond. Hence, we perform molecular dynamics of the cluster with ADMP for better sampling of relative configurations of water in the cluster. Those configurations are then utilized in the scheme above (Section 2) for evaluation of the free energy. The free energies evaluated this way are in excellent agreement with experimental gas phase cluster data (Figure 5). Our scheme (Section 2) is highly effective here because it is applied to the isolated cluster and interactions with only a single surface water molecule are manipulated.

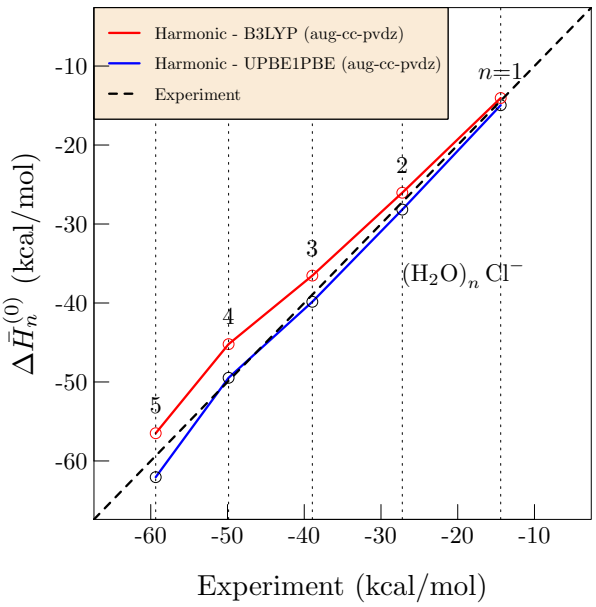



Figure 4: Comparison of harmonic approximation with cluster experiments[68] for $\Delta\bar{H}_n^{(0)}$, the partial molar enthalpy of $(H_2O)_n\,Cl^-$ in the ideal gas phase. Both functionals tested here satisfactorily follow the observed trend. The UPBE1PBE functional, more accurate in this comparison, is adopted as a basis for further QCT analysis of $(H_2O)_n\,Cl^-$.The experimental standard state is the ideal gas at $(T, p) = (298\text{ K}, 1\text{ atm})$.

### *3.3. Comparison with* $(H_2O)_n\,F^-$

In light of the successful treatment of chloride clusters with ADMP, we next take up the case of fluoride. For comparison, the same steps are followed as before (Section 2) to treat the $(H_2O)_n\,F^-$ cluster. Beyond the complication of ligand-ligand H-bonding, we initially note that the hydration structures of $H_2O - F^-$ and $H_2O - Cl^-$ are qualitatively different. In the former case, classic OH-bond donation characterizes the clusters, while in the latter case, more flexible but '*dipole-dominated*' configurations occur (Figure 1). Another interesting observation is that, in contrast to $(H_2O)_n\,Cl^-$, the harmonic approximation satisfactorily predicts free energy in the case of $(H_2O)_n\,F^-$ for $n \leq 4$ (right panel, Figure 5).

These observations on the differences between $Cl^-$ and $F^-$ can be explained as follows. Firstly, spectroscopic studies[103] of halide-water clusters based on Ar predissociation have identified vibrational bands that correspond to inter-water H-bonding. The spectra revealed that those interactions gradually weaken when going from $(H_2O)_2\,I^-$ to $(H_2O)_2\,F^-$ clusters. For $(H_2O)_2\,F^-$, that vibrational band disappears, with water molecules separating entirely. This result is consistent with our geometry optimization calculations for $(H_2O)_2\,F^-$ (Figure 6). The fact that a harmonic approximation reproduces the experimental free energy at 298 K when applied to that minimum energy structure indicates that inter-water H-bonding between waters is not significant in $(H_2O)_n\,F^-$. That argument extends up to $n = 4$ because no H-bond exists in those energy-optimized structures.

Secondly, previous *ab initio* MD work[104] compared the computed IR absorption spectrum for $(H_2O)_6\,Cl^-$ with experimental spectra obtained for $(H_2O)_5\,Cl^-$. That work suggested that accounting for anharmonicity and coupling between modes should be important for the treatment of inter-water H-bond dynamics in aqueous clusters. Here, our step-wise scheme (Section 2) based on the ADMP approach naturally includes those dynamical features. This quantitative treatment addresses the competing inter-water H-bond dynamics in $(H_2O)_n\,Cl^-$ $(n \geq 2)$, leading to cluster free energies in excellent agreement with experiments. The earlier suggestion also explains why the harmonic approximation works well for the case of $(H_2O)\,Cl^-$, where inter-water interactions are absent.

### *3.4. Free Energy of Hydration*

Summing the quasi-chemical components of Eq.(1), we obtain an estimate of the net hydration free energy ($\mu^{(\mathrm{ex})}_{X^-}$, Figure 7). Note that the smallest contribution to the hydration free energy comes from $RT \ln p_{X^-}(n)$, which accounts for heterogeneity in occupancy of the inner solvation shell. For the most probable occupation cases $(n = 4, 5)$, this contribution is inconsequential ($\approx -0.5$ kcal/mol) compared to the others. Next, the inner-shell interactions are built up by augmenting the isolated cluster free energy (evaluated at 1 atm, Figure 5) with $-nRT \ln 1354$, the ligand replacement contribution that accounts for the actual density of ligands available in liquid phase at standard conditions, 1 g/cm$^3$. The full inner shell free energy contribution $\left(-RT \ln K_n^{(0)} {\rho_{H_2O}}^n\right)$ increases in magnitude with $n$. The outer-shell contribution $\left(\mu^{(\mathrm{ex})}_{(H_2O)_n X^-} - n\mu^{(\mathrm{ex})}_{H_2O}\right)$ is treated using the polarizable continuum model (PCM) and decreases in magnitude with $n$. Finally, these contributions balance to produce a hydration free energy that is independent of $n$ (Figure 7). These evaluations agree reasonably well with experimental hydration free energies[105] for $Cl^-$ ($-81.3$ kcal/mol) and $F^-$ ($-111.1$ kcal/mol).

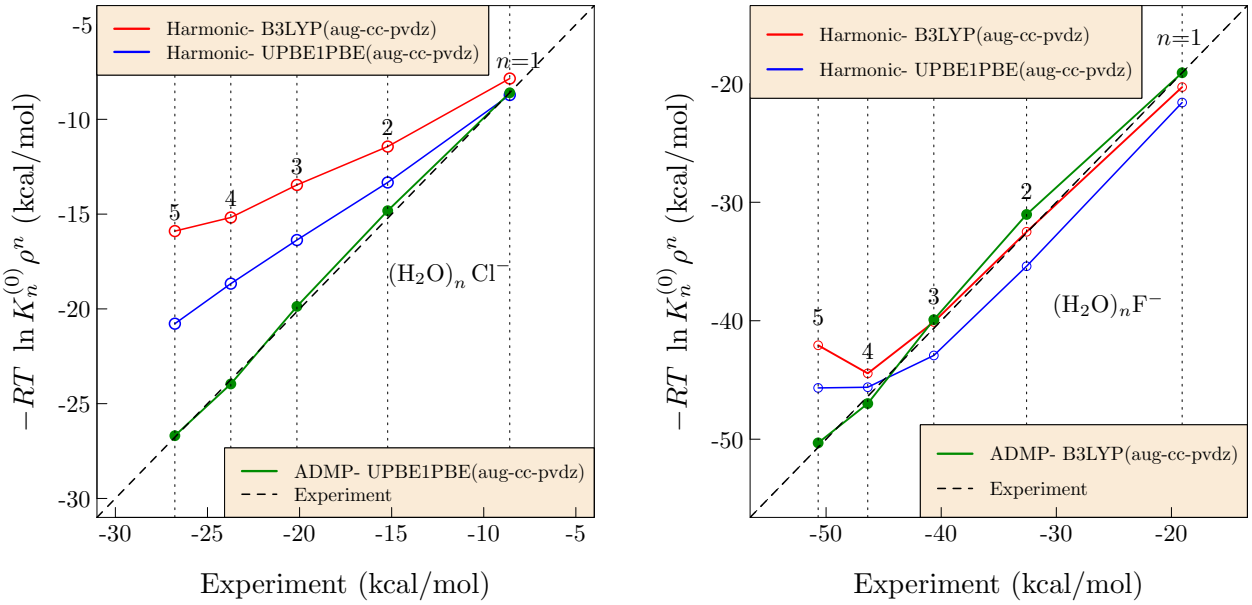



Figure 5: Evaluation of the free energy $-RT\ln K_n^{(0)}\rho^n$ for $(H_2O)_nX^-$ clusters, for $n \leq 5$ (X = Cl or F). The results make explicit the limitation of a harmonic approximation for $(H_2O)_nCl^-$. The fuller analysis of the dynamics of the cluster through ADMP yields excellent comparison with cluster experiments.[68] The experimental standard state is the ideal gas at $(T, p)$ = (298 K,1 atm).

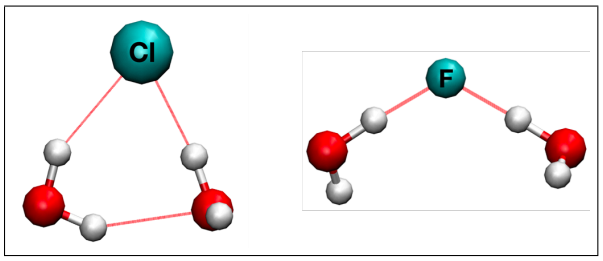



Figure 6: Optimized geometries for $(H_2O)_2\,Cl^-$ and $(H_2O)_2\,F^-$ obtained using UPBE1PBE and B3LYP functionals respectively. The aug-cc-pvdz basis was used in both cases. The $(H_2O)_2\,Cl^-$ cluster includes inter-water H-bonding in contrast to $(H_2O)_2\,F^-$, consistent with (Ar predissociation) spectroscopy studies for halides.[103] A harmonic approximation satisfactorily predicts the free energy for $(H_2O)_2\,F^-$ but not $(H_2O)_2\,Cl^-$.

As an indication of the numerical sensitivity of such calculations, we note a previous QCT treatment that arrived at a value of −228 kcal/mol for the LiF (aq) pair.[37] For comparison, an AIMD calculation based on an electron density functional obtained −240 kcal/mol.[106] These two results bracket experimental values, nearly equally. When the latter result was corrected *ex post facto* by MP2 calculations on a finite solution fragment for the $F^-$ case, the corrected value splits the indicated difference. This comparison suggests the importance of detailed treatment of dispersion effects for anions, though not necessarily for cations.[107]

Since QCT explicitly discriminates between inner- and outer-shell effects, comparison of the different free energy contributions to hydration of $Cl^-$ and $F^-$ leads to some interesting observations (Figure 7). The cluster hydration contributions, $\left(\mu^{(ex)}_{(H_2O)_nX^-} - n\mu^{(ex)}_{H_2O}\right)$, are nearly identical. This quantitatively supports the intuition that long-ranged interactions, predominantly electrostatic, do not discriminate between $Cl^-$ and $F^-$. In contrast, the inner-shell interactions, $-RT\ln K_n^{(0)}{\rho_{H_2O}}^n$, differ by 24 kcal/mol, essentially making up the difference (26.3 kcal/mol) in the hydration free energies. Clearly, disparities in the size and electronic structure of these ions contribute to the differences reported here, but those effects are localized to the inner solvation shell. Thus, the treatment of specific ion effects can focus primarily on accurate evaluation of inner-shell contributions to free energy through rigorous treatment of dynamics in small clusters, as demonstrated here.

## 4. Discussion and Conclusions

These results confirm again that a foremost difficulty in treating hydrated anions such as $Cl^-$(aq) is significant water-water H-bonding within the inner solvation shell (Figure 6). Nevertheless, the hydration structures of *one-water molecule*

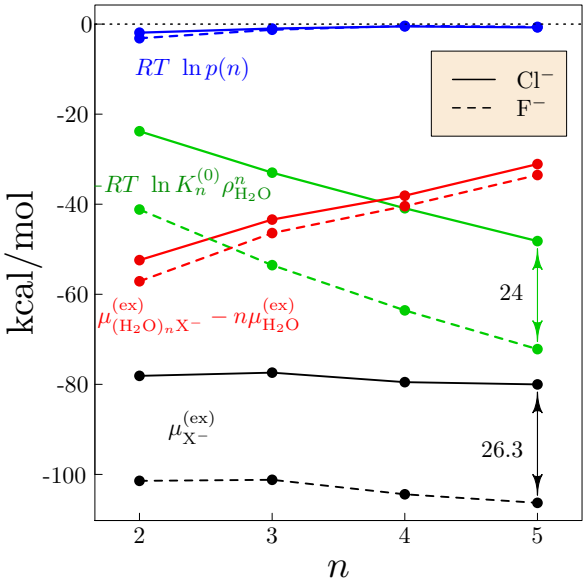



Figure 7: Black: The excess free energy of hydration for $X^-$, evaluated using Eq. (1). Red: The cluster hydration contribution to the hydration free energy evaluated using the PCM model[69] with configurations sampled from ADMP. Green: Isolated cluster free energy from ADMP calculations (Figure 5). Blue: The poly-dispersity contribution obtained from AIMD simulations. Experimental values for the difference, $\mu^{(ex)}_{Cl^-}$ - $\mu^{(ex)}_{F^-}$, are 28 kcal/mol[108] and 29.8 kcal/mol[105] compared to 26.3 kcal/mol here.

cases, $H_2O - F^-$ and $H_2O - Cl^-$, differ qualitatively (Figures 1 and 2), with the latter complex being qualitatively a *dipole-dominated* structure. Of course, this feature facilitates inter-ligand H-bonding for the $Cl^-$(aq) case. The ADMP computational tool works satisfactorily for dynamics of the isolated inner-shell clusters that are treated in QCT. But details of the trajectory thermostat algorithm deserve further elucidation (Supporting Information). A one-ligand stepwise evaluation of the cluster free energies works surprisingly well, and those computational results agree nicely with experimental cluster free energies (Figure 5).

Collection of the several factors contributing to the QCT free energy (Figure 7) produces net results in good agreement with experimental tabulations.[105,108] More decisively, the difference $\mu^{(ex)}_{Cl^-}$ - $\mu^{(ex)}_{F^-}$ is not subject to an ambiguity of a *potential of the phase* (or 'surface potential'). Thermodynamic results then provide an unambiguous test for the difference. Here, the QCT result for the difference is about 2-3 kcal/mol smaller than the experimental value for that difference, about -29 kcal/mol. This discrepancy is likely due to use of the PCM treatment for the cluster-hydration contribution, which treats long-range interactions. Thus, differential outer-shell structuring not considered by PCM is likely a principal contribution to the difference. The AIMD results presented here (Figure 3) characterize that outer-shell structure. Note that the QCT approach uses the PCM approximation in a context where it is insensitive to adjustment of dielectric radii, so the discrepancy identified here is likely to be intrinsic to the PCM model.

The QCT analysis assigns (Figure 7) 90% of the hydration free energy difference $\mu^{(ex)}_{Cl^-}$ - $\mu^{(ex)}_{F^-}$ to inner-shell contributions deriving from the isolated hydrous cluster. This result is an important idea to keep in mind in addressing Hofmeister effects and selectivity of ion channels.[109,110] Precision in analyzing single-ion free energies should assist in understanding selectivity in ion channels by establishing end-point free energies bracketing a path for ion transit.

## 5. Methods

### *5.1. ADMP*

We evaluated molecular dynamics of the isolated $(H_2O)_nCl^-$ clusters for $1 \leq n \leq 5$ using atom-centered basis sets and the density matrix propagation (ADMP) approach[71] available through the Gaussian09 software package.[111] The UPBE1PBE density functional was utilized with the aug-cc-pvdz basis set. The fictitious masses that couple electron motion with the nuclei was set to 0.1 amu. The initial velocities of the individual atoms were sampled randomly from a Boltzmann distribution, and the initial density matrix velocity was chosen to be zero. With a time step of 0.1 fs, dynamic simulations were carried out for 1 ps at 300 K for all cluster sizes, and the last 0.5 ps were used for analysis.

One reservation in using Gaussian09 for dynamics is that description of the only implemented thermostat option has been sketchy.[71] Operationally, this algorithm constrains the total nuclear kinetic energy of the system. Intuitive, non-canonical thermostats are known to cause problems in some cases, as in the flying ice cube effect.[112] Nevertheless, due to lack of alternatives in Gaussian09, we used that thermostat to maintain the system at 300 K.

Though reservations with that thermostat should be borne in mind, they do not appear to be serious here. First, the atomic velocities are verified to be Maxwell-Boltzmann distributed (SI, Figure S2). In addition, we performed 10 ps of

*ab initio* molecular dynamics at 300 K with the Nose-Hoover thermostat[113] for $(H_2O)_2\,Cl^-$ using CP2K.[114] The PBE density functional[115] was utilized with GTH[116] pseudopotentials in the Gaussian and plane wave schemes.[117] Molecularly optimized DZVP-MOLOPT-GTH[118] basis sets were obtained from the CP2K website. The structures sampled by this CP2K trajectory were then analyzed with Gaussian09 using the UPBE1PBE density functional and the aug-cc-pvdz basis set. The isolated cluster free energy obtained this way is within 0.1 kcal/mol of the ADMP trajectory result. A detailed comparison of the cluster simulation methods discussed above is provided with the Supporting Information (SI, Figure S3).

### *5.2. PCM for ADMP sampled clusters*

The outer-shell cluster contribution $\left(\mu^{(\mathrm{ex})}_{(H_2O)_n Cl^-} - n\mu^{(\mathrm{ex})}_{H_2O}\right)$ to the hydration free energy is treated using the polarizable continuum model[69] (PCM) in Gaussian09.[111] Configurations that obey the clustering constraint were extracted from the last 1 ps of the ADMP trajectory. The sampled geometrical structures were subjected to two (2) single point electronic calculations, separately, one for the isolated cluster and a second with the external (dielectric) medium described by the PCM tool. The difference, $\bar{\varepsilon}_j$, is employed in computing

$$\mu^{(\mathrm{ex})}_{(H_2O)_n Cl^-} = -RT \ln \left[ \left( \frac{1}{N} \right) \sum_{j=1}^{N} \mathrm{e}^{-\bar{\varepsilon}_j / RT} \right], \quad (7)$$

where $N$ is the number of configurations from the simulation stream that obey the clustering constraint. Eq. (7) corresponds to the potential distribution theorem (PDT) approach,[28,34] recognizing that thermal fluctuations implicit in the PCM[69] approach complete the PDT averaging.

### *5.3. AIMD*

A system consisting of a single halide ion ($Cl^-$ or $F^-$) and 64 waters was simulated using the VASP AIMD simulation package.[119,120] A wide range of alternative electron density functionals are available, in principal,[121] for such calculations. Here we chose the PW91 generalized gradient approximation principally for consistency with previous calculations.[122] The plane wave basis had a high kinetic energy cutoff of 400 eV.

A cubic cell of 1.24 nm was used to set a satisfactory density of the water. The calculation adopted the Nosé thermostat procedure[113] at 350 K. With respect to the ADMP calculations with $T = 300$ K and with the water density set, that temperature adjustment amounts to a scaling of the potential energy by 300/350. That scaling at constant density avoids glassy behavior that can result otherwise.[123]

A time step of 0.5 fs was chosen to realize a 100 ps trajectory. The last 50 ps were used for analysis. The radial distribution functions, $g_{H|X}(r)$, and the inner-shell occupancy probabilities, $p_{X^-}(n)$, were evaluated on that basis. The radial distribution functions (Figure 3) provide qualitative guidance to the present statistical theory, but not numerical input. The occupancy probabilities, $p_{X^-}(n)$, contribute to Eq. (1) but at the boundary of significance for these studies (Figure 7).

## 6. Acknowledgements

This work was performed, in part, at the Center for Integrated Nanotechnologies, an Office of Science User Facility operated for the U.S. Department of Energy (DOE) Office of Science. The work was supported by Sandia National Laboratories (SNL) LDRD program. SNL is a multimission laboratory managed and operated by National Technology and Engineering Solutions of Sandia, LLC., a wholly owned subsidiary of Honeywell International, Inc., for the U.S. DOE's National Nuclear Security Administration under contract DE-NA-0003525. The views expressed in the article do not necessarily represent the views of the U.S. DOE or the United States Government. LRP thanks Dilip Asthagiri and Diego Gomez for helpful discussions.

## Supporting Information

*Geometry optimizations*

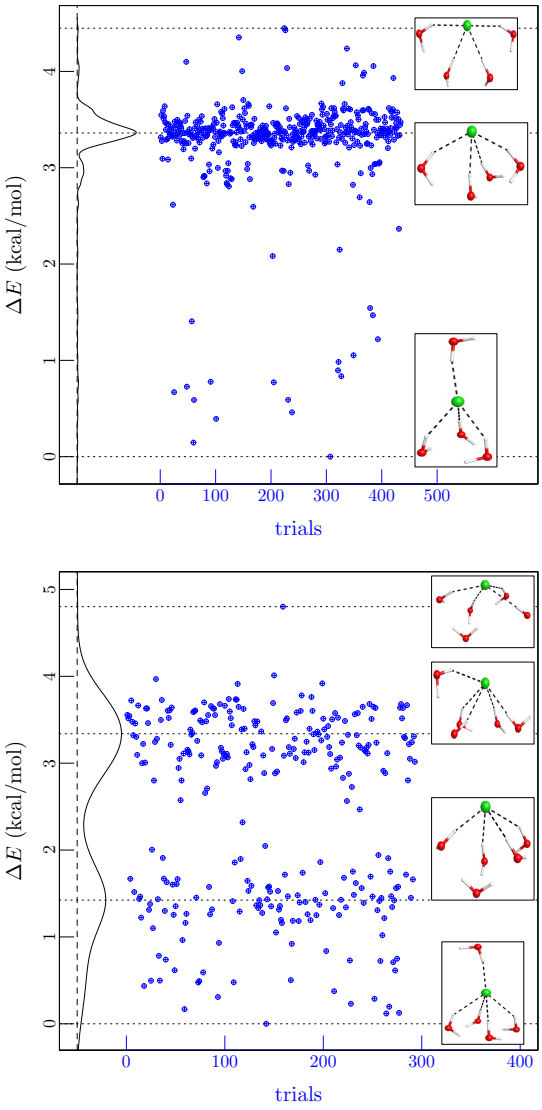



Figure 8: Blue dots: Electronic energy of optimized $(H_2O)_4\,Cl^-$ (left) and $(H_2O)_5\,Cl^-$ (right) clusters with initial configurations sampled from bulk phase AIMD. Black curve on the left shows the distribution of those energies. The lowest optimum energy (bottom inset) is about 4-5 kcal/mol lower in energy than the highest optimum energy (top inset). The harmonic approximation for estimation of cluster free energy is based on the lowest energy optimum. That structure is also used as a starting configuration for molecular dynamics with ADMP.

*Thermostat testing*

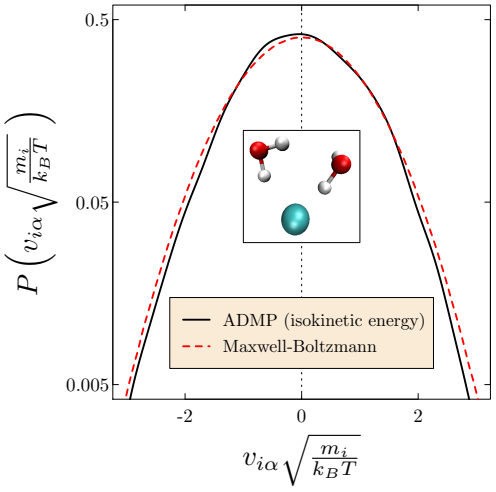



Figure 9: Testing the thermostat implemented with the ADMP approach[71] in the Gaussian09 software package[111] for the cluster $(H_2O)_2\,Cl^-$ at $T$=300 K. The UPBE1PBE density functional was utilized with the aug-cc-pvdz basis set. Variable $\alpha = x, y, z$ indexes the Cartesian components of atomic velocity. The observed distribution of atomic velocities reasonably matches the Maxwell-Boltzmann distribution.

*Comparison of cluster simulation methods*

*Gaussian09 trajectory:*

The ADMP approach utilized the UPBE1PBE density functional with the aug-cc-pvdz basis set. The reservation in using Gaussian09 for dynamics is that the only available thermostat option is not fully described. Nevertheless, the velocity distribution obtained here (Figure 9) matches Maxwell-Boltzmann distribution. For further testing, we use CP2K, as described below.

*CP2K trajectory:*

CP2K allows molecular dynamics with the Nose-Hoover thermostat.[113] The PBE density functional[115] was utilized with pseudopotentials proposed by Goedecker, Teter and Hutter (GTH[116]) in the hybrid Gaussian and plane wave scheme.[117] Molecularly optimized basis sets denoted as DZVP-MOLOPT-GTH[118] were obtained from the CP2K website. The trajectory obtained is then analysed in Gaussian09 using the UPBE1PBE density functional with the aug-cc-pvdz basis set.

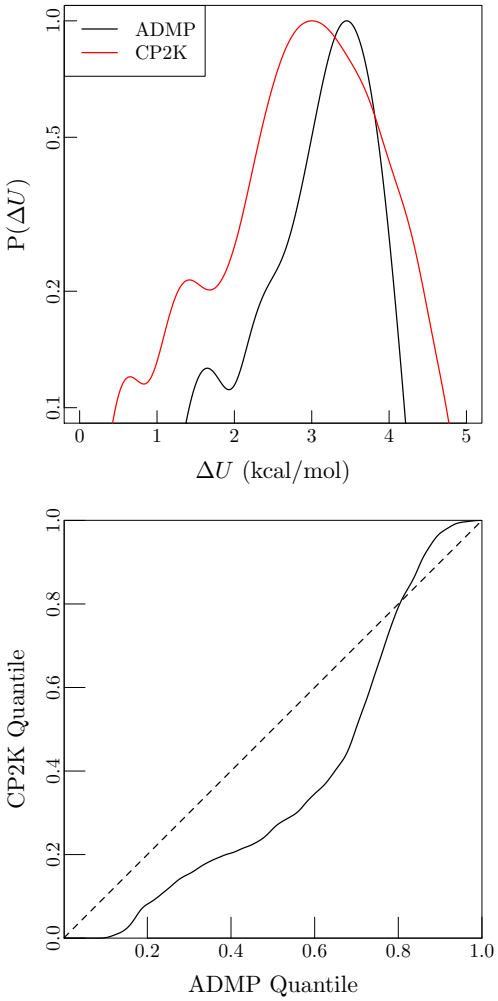



Figure 10: Upper: Comparison of $\Delta U$ samples for $(H_2O)_2\,Cl^-$ obtained using the ADMP approach[71] (black) in the Gaussian09 software package with the mixed Gaussian and plane wave approach (red) in the CP2K package.[114] $\Delta U = E(\gamma_n\sigma) - E(\gamma_{n-1}\sigma) - E(\gamma\sigma) + E(\sigma)$ , defined in the main text. Lower: The standard Q-Q plot for the distribution shown in the left panel.

## References


[1] P. Jungwirth, D. J. Tobias, Specific Ion Effects at the Air/Water Interface, Chem. Rev. 106 (2006) 1259–1281.

[2] I. Kalcher, D. Horinek, R. R. Netz, J. Dzubiella, Ion specific correlations in bulk and at biointerfaces, J. Phys. Cond. Mat. 21 (2009) 424108.

[3] Y. Zhang, P. S. Cremer, Chemistry of Hofmeister Anions and Osmolytes, Annu Rev Phys Chem 61 (2010) 63–83.

[4] W. Kunz, Specific ion effects in colloidal and biological systems, Curr. Op. Coll. & Interf. Sci. 15 (2010) 34–39.

[5] D. F. Parsons, M. Boström, P. L. Nostro, B. W. Ninham, Hofmeister effects: interplay of hydration, nonelectrostatic potentials, and ion size, Phys. Chem. Chem. Phys. 13 (2011) 12352.

[6] T. P. Pollard, T. L. Beck, Toward a quantitative theory of Hofmeister phenomena: From quantum effects to thermodynamics, Curr. Opin. Coll. & Interf. Sci. 23 (2016) 110–118.

[7] N. Sperelakis, Origin of Resting Membrane Potentials, in: Cell Physiology Source Book (Fourth Edition), Academic Press, 2012, pp. 121 – 145.

[8] X. You, M. I. Chaudhari, L. R. Pratt, Comparison of mechanical and thermodynamical evaluations of electrostatic potential differences between electrolyte solutions, in: P. Lo Nostro, B. W. Ninham (Eds.), Aqua Incognita: Why ice floats on water and Gallileo 400 years on, Connor Court Publishing Pty Ltd, 2014, pp. 434–442.

[9] L. R. Pratt, Contact potentials of solution interfaces: phase equilibrium and interfacial electric fields, J. Phys. Chem. 96 (1992) 25–33.

[10] K. Leung, S. B. Rempe, O. A. von Lilienfeld, Ab initio molecular dynamics calculations of ion hydration free energies, J. Chem. Phys. 130 (20) (2009) 204507–204517.

[11] J. Lyklema, Interfacial Potentials: Measuring the Immeasurable?, Substantia 1 (2).

[12] C. C. Doyle, Y. Shi, T. L. Beck, The importance of the water molecular quadrupole for estimating interfacial potential shifts acting on ions near the liquid-vapor interface, The Journal of Physical Chemistry B.

[13] P. Jungwirth, D. J. Tobias, Chloride Anion on Aqueous Clusters, at the Air−Water Interface, and in Liquid Water: Solvent Effects on $Cl^-$ Polarizability, J. Phys. Chem. A 106 (2002) 379–383.

[14] P. Jungwirth, D. J. Tobias, Ions at the Air/Water Interface, J. Phys. Chem. B 106 (2002) 6361–6373.

[15] A. Tongraar, B. Michael Rode, The hydration structures of $F^-$and $Cl^-$ investigated by *ab initio* QM/MM molecular dynamics simulations, Phys. Chem. Chem. Phys. 5 (2003) 357–362.

[16] J. M. Heuft, E. J. Meijer, Density functional theory based molecular-dynamics study of aqueous iodide solvation, J. Chem. Phys. 123 (2005) 094506–6.

[17] J. M. Heuft, E. J. Meijer, Density functional theory based molecular-dynamics study of aqueous fluoride solvation, J. Chem. Phys. 122 (2005) 094501–8.

[18] J. M. Heuft, E. J. Meijer, Density functional theory based molecular-dynamics study of aqueous chloride solvation, J. Chem. Phys. 119 (2003) 11788–11791.

[19] M.-H. Ho, M. L. Klein, I. F. W. Kuo, Bulk and Interfacial Aqueous Fluoride: An Investigation via First Principles Molecular Dynamics, J. Phys. Chem. A 113 (2009) 2070–2074.

[20] S. Raugei, M. L. Klein, An ab initio study of water molecules in the bromide ion solvation shell, J. Chem. Phys. 116 (2002) 196–8.

[21] O. M. Cabarcos, C. J. Weinheimer, J. M. Lisy, S. S. Xantheas, Microscopic hydration of the fluoride anion, J. Chem. Phys. 110 (1999) 5–8.

[22] A. Bankura, V. Carnevale, M. L. Klein, Hydration structure of salt solutions from ab initio molecular dynamics, J. Chem. Phys. 138 (2013) 014501.

[23] L. Perera, M. L. Berkowitz, Structures of $Cl^-(H_2O)_n$ and $F^-(H_2O)_n$ (n=2,3,...,15) clusters. Molecular dynamics computer simulations, J. Chem. Phys. 100 (1994) 3085–3093.

[24] L. S. Sremaniak, L. Perera, M. L. Berkowitz, Enthalpies of formation and stabilization energies of $Br^-(H_2O)_n$ ($n$=1,2,. . . , 15) clusters. Comparisons between molecular dynamics computer simulations and experiments, Chem. Phys. Lett. 218 (1994) 377–382.

[25] D. H. Herce, L. Perera, T. A. Darden, C. Sagui, Surface solvation for an ion in a water cluster, J. Chem. Phys. 122 (2005) 024513–11.

[26] B. L. Eggimann, J. I. Siepmann, Size Effects on the Solvation of Anions at the Aqueous Liquid-Vapor Interface, J. Phys. Chem. C 112 (2007) 210–218.

[27] M. Boström, W. Kunz, B. W. Ninham, Hofmeister effects in surface tension of aqueous electrolyte solution, Langmuir 21 (6) (2005) 2619–2623.

[28] D. Asthagiri, P. Dixit, S. Merchant, M. Paulaitis, L. Pratt, S. B. Rempe, S. Varma, Ion selectivity from local configurations of ligands in solutions and ion channels, Chem. Phys. Lett. 485 (2010) 1–7.

[29] D. M. Rogers, D. Jiao, L. R. Pratt, S. B. Rempe, Structural models and molecular thermodynamics of hydration of ions and small molecules, in: Annu Rep Comput Chem, Vol. 8, Elsevier, 2012, pp. 71–127.

[30] D. M. Rogers, T. L. Beck, Quasichemical and structural analysis of polarizable anion hydration, J. Chem. Phys. 132 (2010) 014505–13.

[31] L. R. Pratt, S. B. Rempe, Quasi-chemical theory and implicit solvent models for simulations, in: Simulation and Theory of Electrostatic Interactions in Solution. Computational Chemistry, Biophysics, and Aqueous Solutions, Vol. 492 of AIP Conference Proceedings, American Institute of Physics, Vol. 492, AIP, 1999, pp. 172–201.

[32] S. B. Rempe, L. R. Pratt, G. Hummer, J. D. Kress, R. L. Martin, A. Redondo, The Hydration Number of $Li^+$ in Liquid Water, J. Am. Chem. Soc. 122 (2000) 966–967.

[33] A. Paliwal, D. Asthagiri, L. R. Pratt, H. S. Ashbaugh, M. E. Paulaitis, An analysis of molecular packing and chemical association in liquid water using quasichemical theory, J. Chem. Phys. 124 (2006) 224502.

[34] T. L. Beck, M. E. Paulaitis, L. R. Pratt, The Potential Distribution Theorem and Models of Molecular Solutions, Cambridge University Press, 2006.

[35] J. Shah, D. Asthagiri, L. Pratt, M. Paulaitis, Balancing local order and long-ranged interactions in the molecular theory of liquid water, J. Chem. Phys. 127 (2007) 144508.

[36] S. Chempath, L. R. Pratt, Distribution of Binding Energies of a Water Molecule in the Water Liquid−Vapor Interface, J. Phys. Chem. B 113 (2009) 4147–4151.

[37] A. Muralidharan, L. R. Pratt, M. I. Chaudhari, S. B. Rempe, Quasi-Chemical Theory With Cluster Sampling From Ab Initio Molecular Dynamics: Fluoride ($F^-$) Anion Hydration, J. Phys. Chem. A 122 (2018) 9806–9812.

[38] L. R. Pratt, H. S. Ashbaugh, Self-consistent molecular field theory for packing in classical liquids, Phys. Rev. E 68 (2003) 021505.

[39] V. Weber, S. Merchant, D. Asthagiri, Communication: Regularizing binding energy distributions and thermodynamics of hydration: Theory and application to water modeled with classical and ab initio simulations, J. Chem. Phys. 135 (2011) 181101.

[40] D. Sabo, S. Rempe, J. Greathouse, M. Martin, Molecular studies of the structural properties of hydrogen gas in bulk water, Mol. Simulat. 32 (3-4) (2006) 269–278.

[41] D. Sabo, S. Varma, M. G. Martin, S. B. Rempe, Studies of the thermodynamic properties of hydrogen gas in bulk water, J. Phys. Chem. B 112 (3) (2008) 867–876.

[42] J. S. Clawson, R. T. Cygan, T. M. Alam, K. Leung, S. B. Rempe, Ab initio study

of hydrogen storage in water clathrates, J. Comput. Theor. Nanosci. 7 (12) (2010) 2602–2606.

[43] D. Jiao, S. B. Rempe, Combined density functional theory (DFT) and continuum calculations of p$K_a$ in carbonic anhydrase, Biochem. 51 (30) (2012) 5979–5989.

[44] D. Jiao, S. B. Rempe, $CO_2$ Solvation Free Energy Using Quasi-Chemical Theory, J. Chem. Phys. 134 (2011) 224506.

[45] M. I. Chaudhari, D. Sabo, L. R. Pratt, S. B. Rempe, Hydration of Kr(aq) in Dilute and Concentrated Solutions, J. Phys. Chem. B 119 (2015) 9098–9102.

[46] S. Varma, S. B. Rempe, Tuning ion coordination architectures to enable selective partitioning, Biophys. J. 93 (4) (2007) 1093 – 1099.

[47] S. Varma, D. M. Rogers, L. R. Pratt, S. B. Rempe, Design principles for $K^+$ selectivity in membrane transport, J. Gen. Physiol. 137 (2011) 479–488.

[48] D. M. Rogers, S. B. Rempe, Probing the thermodynamics of competitive ion binding using minimum energy structures, J. Phys. Chem. B 115 (29) (2011) 9116–9129.

[49] M. I. Chaudhari, S. B. Rempe, Strontium and barium in aqueous solution and a potassium channel binding site, J. Chem. Phys. 148 (2018) 222831.

[50] S. Varma, D. Sabo, S. B. Rempe, $K^+/Na^+$ selectivity in K channels and valinomycin: Over-coordination versus cavity-size constraints, J. Mol. Biol. 376 (1) (2008) 13 – 22.

[51] M. I. Chaudhari, L. R. Pratt, M. E. Paulaitis, Concentration dependence of the Flory-Huggins interaction parameter in aqueous solutions of capped PEO chains, J. Chem. Phys. 141 (2014) 244908–5.

[52] M. J. Stevens, S. L. Rempe, Ion-specific effects in carboxylate binding sites, J. Phys. Chem. B 120 (49) (2016) 12519–12530.

[53] S. B. Rempe, L. R. Pratt, The hydration number of $Na^+$ in liquid water, Fluid Phase Equilib. 183 (2001) 121–132.

[54] D. Asthagiri, L. R. Pratt, Quasi-chemical study of $Be^{2+}$(aq) speciation, Chem. Phys. Lett. 371 (2003) 613–619.

[55] S. B. Rempe, D. Asthagiri, L. R. Pratt, Inner shell definition and absolute hydration free energy of $K^+$(aq) on the basis of quasi-chemical theory and ab initio molecular dynamics, Phys. Chem. Chem. Phys. 6 (8) (2004) 1966–1969.

[56] D. Asthagiri, L. R. Pratt, M. E. Paulaitis, S. B. Rempe, Hydration structure and free energy of biomolecularly specific aqueous dications, including $Zn^{2+}$ and first transition row metals, J. Am. Chem. Soc. 126 (4) (2004) 1285–1289.

[57] S. Varma, S. B. Rempe, Structural transitions in ion coordination driven by changes in competition for ligand binding, J. Am. Chem. Soc. 130 (46) (2008) 15405–15419.

[58] D. Jiao, K. Leung, S. B. Rempe, T. M. Nenoff, First principles calculations of atomic nickel redox potentials and dimerization free energies: A study of metal nanoparticle growth, J. Chem. Theory Comput. 7 (2) (2010) 485–495.

[59] D. Sabo, D. Jiao, S. Varma, L. R. Pratt, S. B. Rempe, Case Study of $Rb^+$(aq), Quasi-Chemical Theory of Ion Hydration, and the No Split Occupancies Rule, Ann. Rep. Prog. Chem, Sect. C (Phys. Chem.) 109 (2013) 266–278.

[60] M. I. Chaudhari, M. Soniat, S. B. Rempe, Octa-coordination and the aqueous $Ba^{2+}$ ion, J. Phys. Chem. B 119 (28) (2015) 8746–8753.

[61] M. I. Chaudhari, J. R. Nair, L. R. Pratt, F. A. Soto, P. B. Balbuena, S. B. Rempe, Scaling atomic partial charges of carbonate solvents for lithium ion solvation and diffusion, J. Chem. Theory Comput. 12 (12) (2016) 5709–5718.

[62] M. I. Chaudhari, L. R. Pratt, S. B. Rempe, Utility of chemical computations in predicting solution free energies of metal ions, Mol. Sim. 44 (2018) 110–116.

[63] V. Weber, D. Asthagiri, Regularizing binding energy distributions and the hydration free energy of protein cytochrome C from

all-atom simulations, J. Chem. Theory & Comp. 8 (9) (2012) 3409–3415.

[64] D. S. Tomar, D. Asthagiri, V. Weber, Solvation Free Energy of the Peptide Group: Its Model Dependence and Implications for the Additive-Transfer Free-Energy Model of Protein Stability, Biophys. J. 105 (2013) 1482–1490.

[65] M. Arshadi, R. Yamdagni, P. Kebarle, Hydration of the halide negative ions in the gas phase. II. Comparison of hydration energies for the alkali positive and halide negative ions, J. Phys. Chem. 74 (1970) 1475–1482.

[66] R. G. Keesee, N. Lee, A. Castleman Jr, Properties of clusters in the gas phase: V. complexes of neutral molecules onto negative ions, J. Chem. Phys. 73 (1980) 2195–2202.

[67] K. Hiraoka, S. Mizuse, S. Yamabe, Solvation of halide ions with $H_2O$ and $CH_3CN$ in the gas phase, J. Phys. Chem. 92 (1988) 3943–3952.

[68] M. D. Tissandier, K. A. Cowen, W. Y. Feng, E. Gundlach, M. H. Cohen, A. D. Earhart, J. V. Coe, T. R. Tuttle, The proton's absolute aqueous enthalpy and gibbs free energy of solvation from cluster-ion solvation data, J. Phys. Chem. A 102 (1998) 7787–7794.

[69] J. Tomasi, B. Mennucci, R. Cammi, Quantum Mechanical Continuum Solvation Models, Chem. Rev. 105 (2005) 2999–3093, Note Eq. (74) and the following discussion regarding the factor of "1/2" introduced there.

[70] D. Marx, J. Hutter, Ab initio molecular dynamics: Theory and implementation, Modern Methods and Algorithms of Quantum Chemistry 1 (301-449) (2000) 141.

[71] H. B. Schlegel, S. S. Iyengar, X. Li, J. M. Millam, G. A. Voth, G. E. Scuseria, M. J. Frisch, Ab initio molecular dynamics: Propagating the density matrix with Gaussian orbitals. iii. comparison with born–oppenheimer dynamics, J. Chem. Phys. 117 (2002) 8694–8704.

[72] F. J. Alvarez-Leefmans, E. Delpire, Physiology and Pathology of Chloride Transporters and Channels in the Nervous System: From Molecules to Diseases, Academic Press, 2009.

[73] E. Park, E. B. Campbell, R. MacKinnon, Structure of a CLC chloride ion channel by cryo-electron microscopy, Nature 541 (2017) 500.

[74] T. J. Jentsch, V. Stein, F. Weinreich, A. a. Zdebik, Molecular structure and physiological function of chloride channels, Physiol. Rev. 82 (2002) 503–568.

[75] J. L. Robertson, L. Kolmakova-Partensky, C. Miller, Design, function and structure of a monomeric CLC transporter, Nature 468 (2010) 844.

[76] A. Accardi, A. Picollo, CLC channels and transporters: Proteins with borderline personalities, Biochim. Biophys. Acta - Biomembranes 1798 (2010) 1457–1464.

[77] R. B. Stockbridge, L. Kolmakova-Partensky, T. Shane, A. Koide, S. Koide, C. Miller, S. Newstead, Crystal structures of a double-barrelled fluoride ion channel, Nature 525 (2015) 548.

[78] I. Shrivastava, P. Tieleman, P. C. Biggin, M. Sansom, $K^+$ versus $Na^+$ ions in a K channel selectivity filter: A simulation study, Biophys. J. 83 (2002) 633–645.

[79] M. Thomas, D. Jayatilaka, B. Corry, The predominant role of coordination number in potassium channel selectivity, Biophys. J. 93 (8) (2007) 2635 – 2643.

[80] D. L. Bostick, C. L. Brooks, Selectivity in $K^+$ channels is due to topological control of the permeant ion's coordinated state, Proc. Natl. Acad. Sci., U.S.A. 104 (22) (2007) 9260–9265.

[81] P. Fowler, K. Tai, M. Sansom, The selectivity of $K^+$ ion channels: Testing the hypotheses, Biophys. J. 95 (2008) 5062–5072.

[82] D. L. Bostick, C. L. Brooks III, Statistical determinants of selective ionic complexation: ions in solvent, transport proteins, and other hosts, Biophys. J. 96 (11) (2009) 4470–4492.

[83] B. Roux, S. Bernèche, B. Egwolf, B. Lev, S. Y. Noskov, C. N. Rowley, H. Yu, Ion selectivity in channels and transporters, J. Gen. Physiol. 137 (2011) 415–426.

[84] S. Y. Noskov, B. Roux, Importance of hydration and dynamics on the selectivity of the KcsA and NaK channels, J. Gen. Physiol. 138 (2011) 651–651.

[85] P. D. Dixit, D. Asthagiri, Thermodynamics of ion selectivity in the KcsA $K^+$ channel, J. Gen. Physiol. 137 (2011) 427–433.

[86] I. Kim, T. W. Allen, On the selective ion binding hypothesis for potassium channels, Proc. Natl. Acad. Sci., U.S.A. 108 (44) (2011) 17963–17968.

[87] S. Furini, C. Domene, Selectivity and permeation of alkali metal ions in $K^+$-channels, J. Mol. Biol. 409 (5) (2011) 867 – 878.

[88] O. S. Andersen, Perspectives on: Ion selectivity, J. Gen. Physiol. 137 (2011) 393–395.

[89] A. Alam, Y. Jiang, Structural studies of ion selectivity in tetrameric cation channels, J. Gen. Physiol. 137 (5) (2011) 397–403.

[90] C. M. Nimigean, T. W. Allen, Origins of ion selectivity in potassium channels from the perspective of channel block, J. Gen. Physiol. 137 (5) (2011) 405–413.

[91] D. Medovoy, E. Perozo, B. Roux, Multi-ion free energy landscapes underscore the microscopic mechanism of ion selectivity in the KcsA channel, Biochim. Biophys. Acta Biomembr. 1858 (7, Part B) (2016) 1722 – 1732.

[92] W. Kopec, D. Kopfer, O. Vickery, A. S. Bondarenko, T. L. C. Jansen, B. L. de Groot, U. Zachariae, Direct knock-on of desolvated ions governs strict ion selectivity in $K^+$ channels, Nat. Chem. 10 (2018) 813–820.

[93] F. L. Gervasio, M. Parrinello, M. Ceccarelli, M. L. Klein, Exploring the gating mechanism in the ClC chloride channel via metadynamics, J. Mol. Bio. 361 (2006) 390–398.

[94] Y. J. Ko, W. H. Jo, Chloride ion conduction without water coordination in the pore of ClC protein, J. Comp. Chem. 31 (2010) 603–611.

[95] Z. Kuang, A. Liu, T. L. Beck, Transpath: A computational method for locating ion transit pathways through membrane proteins, Proteins: Structure, Function, and Bioinformatics 71 (2008) 1349–1359.

[96] J. Yin, Z. Kuang, U. Mahankali, T. L. Beck, Ion transit pathways and gating in ClC chloride channels, Proteins: Structure, Function, and Bioinformatics 57 (2004) 414–421.

[97] M. Smith, H. Lin, Charge delocalization upon chloride ion binding in ClC chloride ion channels/transporters, Chem. Phys. Lett. 502 (1-3) (2011) 112–117.

[98] Z. Chen, T. L. Beck, Free energies of ion binding in the bacterial ClC-Ec1 chloride transporter with implications for the transport mechanism and selectivity, J. Phys. Chem. B B 120 (2016) 3129–3139.

[99] M. H. Cheng, R. D. Coalson, Molecular dynamics investigation of $Cl^-$ and water transport through a eukaryotic ClC transporter, Biophys. J. 102 (2012) 1363–1371.

[100] P. C. Jordan, New and Notable: Tuning a potassium channel–the caress of the surroundings, Biophys. J. 93 (4) (2007) 1091–1092.

[101] M. I. Chaudhari, J. Vanegas, A. Muralidharan, L. R. Pratt, S. B. Rempe, Biomolecular hydration mimicry in ion permeation through membrane channels, Acc. Chem. Res.

[102] M. I. Chaudhari, S. B. Rempe, L. R. Pratt, Quasi-chemical theory of $F^-$(aq): The no split occupancies rule revisited, J. Chem. Phys. 147 (2017) 161728.

[103] W. H. Robertson, M. A. Johnson, Molecular aspects of halide ion hydration: The cluster approach, Ann. Rev. Phys. Chem. 54 (2003) 173–213.

[104] D. J. Tobias, P. Jungwirth, M. Parrinello, Surface solvation of halogen anions in water clusters: An ab initio molecular dynamics study of the $Cl^-(H_2O)_6$ complex, J. Chem. Phys. 114 (2001) 7036–7044.

[105] Y. Marcus, A Simple Empirical Model Describing the Thermodynamics of Hydration of Ions of Widely Varying Charges, Sizes, and Shapes, Biophys. Chem. 51 (1994) 111–127.

[106] T. T. Duignan, M. D. Baer, G. K. Schenter, C. J. Mundy, Real single ion solvation free energies with quantum mechanical simulation, Chem. Sci. 8 (2017) 6131–6140.

[107] M. Soniat, D. M. Rogers, S. B. Rempe, Dispersion- and Exchange-Corrected Density Functional Theory for Sodium Ion Hydration, J. Chem. Theory and Comput. (2015) 150626121718001.

[108] H. Friedman, C. Krishnan, Thermodynamics of ionic hydration, in: Aqueous Solutions of Simple Electrolytes, Springer, 1973, pp. 1–118.

[109] S. Merchant, D. Asthagiri, Thermodynamically dominant hydration structures of aqueous ions, J. Chem. Phys. 130 (2009) 195102–11.

[110] S. Y. Willow, S. S. Xantheas, Molecular-Level Insight of the Effect of Hofmeister Anions on the Interfacial Surface Tension of a Model Protein, J. Phys. Chem. Letts. 8 (7) (2017) 1574–1577.

[111] M. Frisch, G. Trucks, H. Schlegel, G. Scuseria, M. Robb, J. Cheeseman, G. Scalmani, V. Barone, B. Mennucci, G. Petersson, Others, Gaussian 09 revision d. 01, 2009, Gaussian Inc. Wallingford CT.

[112] S. C. Harvey, R. K.-Z. Tan, T. E. Cheatham III, The flying ice cube: Velocity rescaling in molecular dynamics leads to violation of energy equipartition, J. Comp. Chem. 19 (1998) 726–740.

[113] S. Nosé, A Molecular Dynamics Method for Simulations in the Canonical Ensemble, Mol. Phys. 52 (1984) 255–268.

[114] J. VandeVondele, M. Krack, F. Mohamed, M. Parrinello, T. Chassaing, J. Hutter, Quickstep: Fast and accurate density functional calculations using a mixed gaussian and plane waves approach, Comp. Phys. Comm. 167 (2005) 103–128.

[115] J. P. Perdew, K. Burke, M. Ernzerhof, Generalized gradient approximation made simple, Phys. Rev. Letts. 77 (1996) 3865.

[116] S. Goedecker, M. Teter, J. Hutter, Separable dual-space Gaussian pseudopotentials, Phys. Rev. B 54 (1996) 1703.

[117] G. Lippert, J. Hutter, M. Parrinello, The Gaussian and augmented-plane-wave density functional method for ab initio molecular dynamics simulations, Theo. Chem. Accts. 103 (1999) 124–140.

[118] J. VandeVondele, J. Hutter, Gaussian basis sets for accurate calculations on molecular systems in gas and condensed phases, J. Chem. Phys. 127 (2007) 114105.

[119] G. Kresse, J. Hafner, Ab initio molecular dynamics for liquid metals, Phys. Rev.B 47 (1993) 558.

[120] G. Kresse, J. Furthmüller, Efficient iterative schemes for ab initio total-energy calculations using a plane-wave basis set, Phys. Rev. B 54 (1996) 11169.

[121] M. J. Gillan, D. Alfè, A. Michaelides, Perspective: How good is DFT for water?, J. Chem. Phys. 144 (2016) 130901–34.

[122] M. I. Chaudhari, L. R. Pratt, S. B. Rempe, Utility of chemical computations in predicting solution free energies of metal ions, Mole. Sim. 492 (2017) 1–7.

[123] S. B. Rempe, T. R. Mattsson, K. Leung, On "The Complete Basis Set Limit" and plane-wave methods in first-principles simulations of water, Phys. Chem. Chem. Phys 10 (2008) 4685–4687.